View Article Online / Journal Homepage / Table of Contents for this issue

NJC

New Journal of Chemistry

A journal for new directions in chemistry

www.rsc.org/njc

Volume 36 | Number 7 | July 2012 | Pages 1425–1528

Published on 02 April 2012. Downloaded by Western Kentucky University on 28/10/2014 22:23:45.

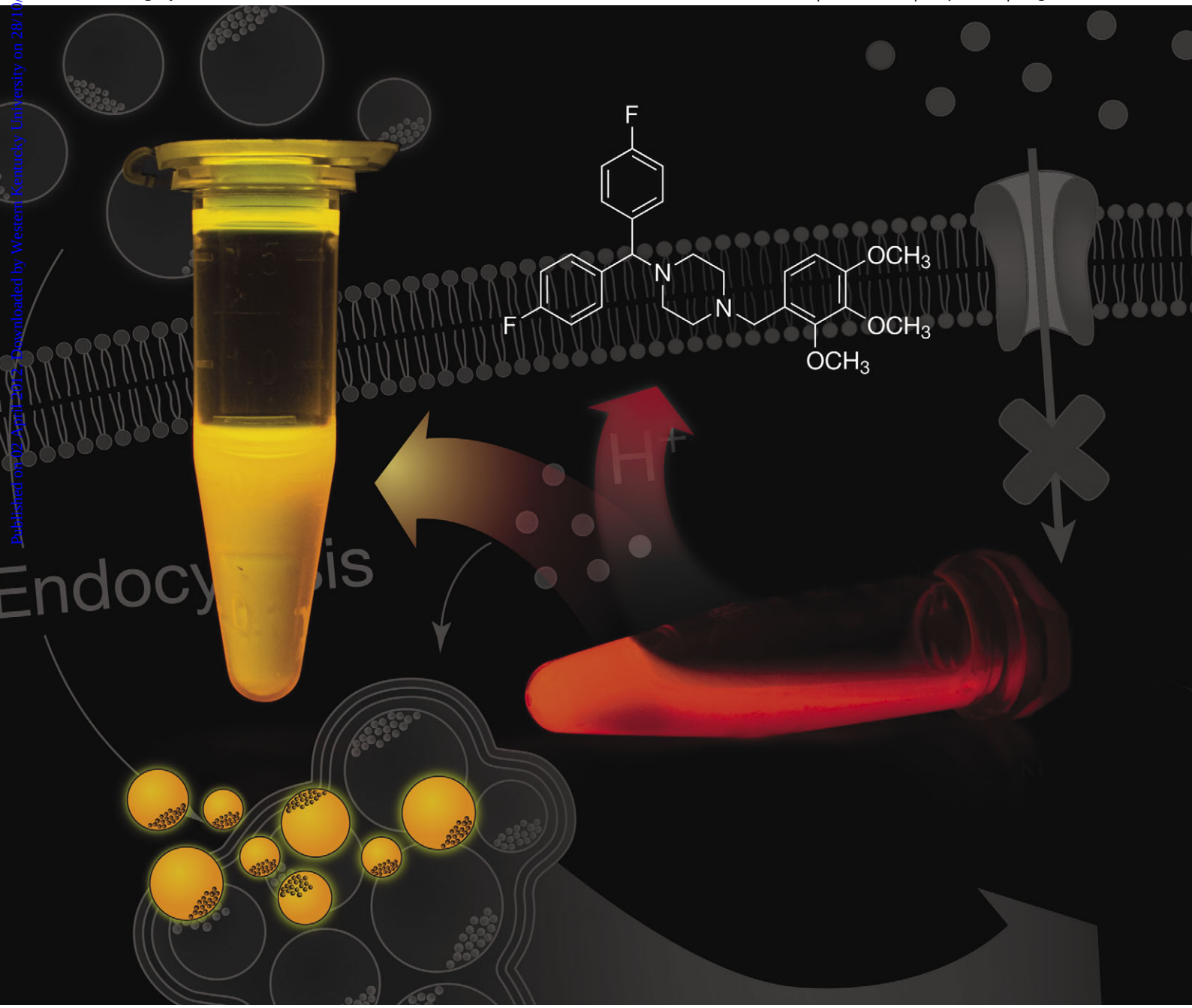

ISSN 1144-0546

RSC Publishing

cnrs

COVER ARTICLE

Iyer *et al.*

Multimodal and multifunctional stealth polymer nanospheres for sustained drug delivery

NJC

View Article Online
Dynamic Article Links

Cite this: *New J. Chem.*, 2012, **36**, 1457–1462

www.rsc.org/njc

PAPER

Multimodal and multifunctional stealth polymer nanospheres for sustained drug delivery†

Cameron W. Evans,[ab] Melissa J. Latter,[a] Diwei Ho,[ab] Saquib Ahmed M. A. Peerzade,[a] Tristan D. Clemons,[ab] Melinda Fitzgerald,[b] Sarah A. Dunlop[b] and K. Swaminathan Iyer*[b]

Received (in Montpellier, France) 9th January 2012, Accepted 24th March 2012
DOI: 10.1039/c2nj40016b

We report the preparation of fluorescent and magnetic PMMA nanospheres, and a corresponding PEGylated 'stealth' analogue prepared using a block copolymer. The nanospheres contain encapsulated magnetite nanoparticles and fluorescent BODIPY dyes, including a new such dye with pH-sensitive fluorescent emission. The new dye could potentially be used as an indicator of the immediate physiological environment. The nanospheres were non-toxic at up to 500 μg ml^{-1} in PC12 cells. Lomerizine, a lipophilic calcium channel blocker, was also encapsulated in the nanospheres and displayed sustained, pH-dependent release characteristics. The nanospheres may be of use to release lomerizine and other water-insoluble drugs at central nervous system injury sites.

Published on 02 April 2012. Downloaded by Western Kentucky University on 28/10/2014 22:23:45.

Introduction

Colloidal systems, including nanoparticles and liposomes, have been extensively studied as potential drug carriers for targeted or controlled release. The encapsulation of drugs in nanoparticles offers one means for controlled or targeted release, but the use of nanosystems could be increased if tracking methods in the body were also incorporated to visualise delivery. For this reason, there is considerable interest in developing multifunctional nanoparticles, which combine imaging and therapy in a single construct.[1] Monitoring of the nano-assembly will facilitate an indirect determination of the site at which the therapy is administered.[2]

It is possible to incorporate more than one imaging tool in a single nanoparticle system, producing a multifunctional particle that supports several imaging modalities. One common combination of imaging modalities is magnetic resonance imaging (MRI) and fluorescence microscopy, which combines the radiation-free, whole-body, deep tissue imaging ability of MRI with the sensitivity of fluorescence detection.[3–7] Delivering drugs using this kind of nanoparticle as the vehicle has several benefits; encapsulated drugs are protected on their journey to the target tissue,[8] and the resulting particles can be followed at the scales of systems and organs by MRI, or at the cellular level by fluorescence.[3,9] Furthermore, the physical encapsulation approach is suited to a variety of molecular and nanoparticulate cargoes without needing substantial modifications to the preparative procedure for the carrier nanoparticles.

Nanoparticles and liposomes are known to be rapidly cleared from tissues and blood by cells of the mononuclear phagocytic system (MPS), particularly macrophages in the liver and spleen[10] (including hepatic Kupffer cells)[11,12] and circulating monocytes.[13] Nanoparticle removal by the MPS occurs by interaction of the hydrophobic surface of particles with plasma proteins (opsonins), which are recognised by specific receptors on macrophages, promoting the binding and phagocytosis of these carriers.[11,13] This is the primary mechanism by which the organs of the reticuloendothelial system (RES)—principally the liver, spleen and bone marrow—recognise circulating nanoparticles.[12]

Nanoparticle clearance by the RES is known to be affected by size and surface characteristics.[13,14] For example, nanoparticles with a hydrophobic surface are removed from circulation more rapidly than those with hydrophilic and neutral surfaces.[13] Previous studies demonstrate that the rate of opsonisation of nanoparticles can be reduced by modifying the nanoparticle surface with a hydrophilic, flexible, and non-ionic polymer.[15] Examples include poly(ethylene glycol) (PEG), polysaccharides, or poloxamers and poloxamines,[10,11] which provide a steric barrier on the particle surface that minimises opsonisation.[12] Nanoparticles that have been modified in this way are typically known as "stealth" particles, because they escape the surveillance of the RES.[12] Increased blood lifetimes of injected nanoparticles

[a] *School of Chemistry and Biochemistry, The University of Western Australia, 35 Stirling Hwy, Crawley WA 6009, Australia. E-mail: swaminatha.iyer@uwa.edu.au; Fax: +61 8 6488 7330; Tel: +61 8 6488 4470*
[b] *Experimental and Regenerative Neurosciences, School of Animal Biology, University of Western Australia, 35 Stirling Hwy, Crawley WA 6009, Australia*

† Electronic supplementary information (ESI) available: TEM of magnetite nanoparticles, magnetic characterisation by SQUID, relaxometry plots. See DOI: 10.1039/c2nj40016b

View Article Online

Published on 02 April 2012. Downloaded by Western Kentucky University on 28/10/2014 22:23:45.

have been related to the presence of PEG on their surfaces.[11,14] Similarly, a PEG corona has been shown to impart a stealth property to liposomes, suppressing recognition and uptake by the RES and extending the circulation time of the particles in the body.[16] Importantly, high concentrations of PEG on the surface alone do not lead to low uptake; the spatial configuration and freedom of the PEG chains is also important.[14] In particular, block copolymers containing a PEG segment have been shown to be very effective at preventing uptake.[14]

Herein, we report a stealth carrier for sustained drug release, using PEG-modified PMMA nanoparticles that contain both magnetite and a fluorescent probe. Using a novel, pH-sensitive BODIPY dye we also show that the emission of the fluorophore can be potentially used as an indicator of the immediate physiological environment. We show that the distribution and loading of magnetite nanoparticles inside these nanocarriers can be regulated by the choice of solvents. Finally, we demonstrate that these stealth nanocarriers can be used as a pH-responsive release agent using lomerizine, a small-molecule drug that is generally insoluble in aqueous systems.

Results and discussion

The BODIPY (4,4-difluoro-4-bora-3a,4a-diaza-*s*-indacene) fluorophores are a popular choice for various sensing and imaging applications. These dyes typically have small Stokes shifts and narrow emission spectra,[17] but most compounds of this class are insoluble in water and emit in the green part of the spectrum, limiting their biological use. On the other hand, methods that increase the versatility of this dye class have been recently reported,[17–24] including strategies to impart water solubility[18–21] and modifications to shift the emission[22–24] (for example, by incorporating chromophores to extend conjugation within the structure).

In this work, two such dyes were synthesised: the green-fluorescent 1,3,5,7,8-pentamethyl BODIPY **3**[25] and the new 1,3,7,8-tetramethyl-5-(4-dimethylaminostyryl) analogue **4**. The parent dye **3** was prepared in one pot by condensation of pyrrole **1** and acid chloride **2** prior to coordination with boron trifluoride-etherate (Scheme 1). Knoevenagel reaction of **3** in the presence of the aldehyde afforded the new dye **4**. Extending the conjugation red-shifted the peak absorption wavelength (λ_{max} 591 nm for **4** in dichloromethane compared to λ_{max} 499 nm for **3** in chloroform[25]), producing a dye that was purple in dichloromethane, while also providing an acid-sensitive group that opens the possibility for sensing behaviour (peak emission wavelength $\lambda_{em} \approx 500$ nm protonated, 670 nm deprotonated). This qualitative reversible molecular switching of BODIPY **4** was also demonstrated in the presence of acid or base (Fig. 1a) as previously seen for the structurally similar *meso*-phenyl BODIPY dye.[26]

Iron oxide nanoparticles (with sizes 4–10 nm) were prepared *via* the high temperature decomposition of $Fe(acac)_3$ (Fig. S1).[27,28] Polymer nanospheres were synthesised from either poly(methyl methacrylate) (PMMA), to give unmodified nanospheres, or from poly(methyl methacrylate)-*block*-poly(ethylene glycol) (PMMA-*b*-PEG) to produce a PEGylated stealth analogue. By including BODIPY dyes and iron oxide nanoparticles in the organic phase, we prepared magnetic and fluorescent polymer nanospheres as

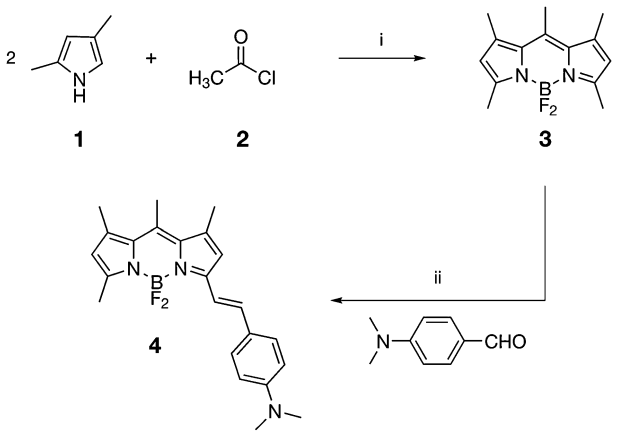

Scheme 1 Preparation of BODIPY dyes **3** and **4**: (i) dichloromethane, triethylamine, boron trifluoride etherate; (ii) toluene, piperidine, acetic acid, molecular sieves.

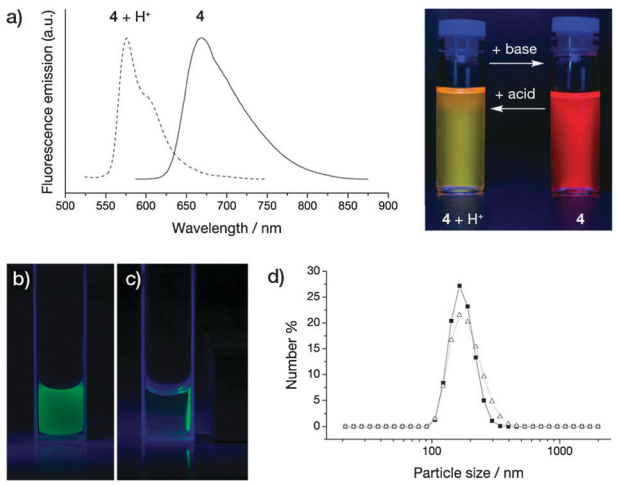

Fig. 1 (a) Fluorescence spectra of **4** (solid) and **4** + H^+ (dashed) recorded in CH_2Cl_2; both spectra have been normalised to give the same maximum emission intensity. The photograph, under UV illumination, shows the colour change observed upon the addition of acid or base; (b) Nanosphere sample (containing BODIPY **3**) dispersed in water; (c) the same sample collected using a permanent magnet; (d) Dynamic light scattering characterisation of nanoparticle size for PMMA (solid) and PMMA-*b*-PEG (open) nanoparticles.

shown in Fig. 1b–c. Nanospheres contained multiple iron oxide nanoparticles; the association of individual magnetite nanoparticles into clusters has been used to increase the transverse relaxivity of nanospheres of the same size while maintaining the superparamagnetic characteristics.[29] The nanospheres produced by this method were stable in aqueous dispersion, even though the iron oxide and BODIPY constituents were not. DLS of the nanospheres showed that the particle size was in the range 100–300 nm, with an average size of approximately 170 nm (Fig. 1d). SQUID data (Fig. S2 and S3) show that the nanospheres maintained the superparamagnetic behaviour of the constituent iron oxide nanoparticles, as indicated by the absence of hysteresis at 300 K and the coincidence of the zero field-cooled and field-cooled magnetisation curves. The FT-IR spectrum of the prepared nanospheres strongly resembled that of PMMA

 This journal is © The Royal Society of Chemistry and the Centre National de la Recherche Scientifique 2012

View Article Online

Published on 02 April 2012. Downloaded by Western Kentucky University on 28/10/2014 22:23:45.

(3000–2800 cm^{-1}, C–H stretch; 1731 cm^{-1}, C=O stretch),[30] and suggested that the unmodified PMMA nanospheres were not substantially PEGylated by the Pluronic surfactant used in the preparation.

The assembly of the magnetite nanoparticles (either uniformly dispersed throughout the nanosphere or selectively associated to one side) could be controlled by changing the solvent mixture employed in the organic phase. The selection of solvents affects the dispersability of the iron oxide nanoparticles within the solvated polymeric micelle, which determines the distribution of these particles within the nanospheres (Fig. 2). The PMMA nanospheres prepared using different solvent mixtures as shown in Fig. 2 had longitudinal relaxivity $r_1 \approx 8\ s^{-1}\ mM^{-1}$ and transverse relaxivity $r_2 \approx 300\ s^{-1}\ mM^{-1}$ as detailed in Fig. S4. The high value of r_2 is similar to other values reported in the literature and confirms the suitability of PMMA nanospheres for use as an MRI contrast agent.[31]

Using a similar technique, drug-loaded nanoparticles were prepared by dissolving lomerizine in the organic phase. Lomerizine is an L- and T-type voltage-gated calcium channel blocker and selective cerebral vasodilator.[32] It protects retinal ganglion cells following optic nerve injury[33–36] and displays neuroprotective effects in a number of other injury models.[37–40] In *in vivo* studies, however, large and repeated doses of lomerizine are used.[33–36] Because injury to the central nervous system results in an extracellular pH drop,[41,42] a pH-responsive, controlled-release drug delivery system will likely be of therapeutic value, delivering greater doses of lomerizine to the most acidic sites. In these kinds of injuries, immune responses can include macrophage recruitment and microglial activation;[33–35] a stealth delivery mechanism may be beneficial if delivery to these sites is desired.

For drug loading, the aqueous phase and subsequent washes were buffered at pH 9 to prevent dissolution of lomerizine during purification. Drug release data were subsequently recorded at pH 5, 6, or 7.4 after magnetic separation of nanoparticles and resuspension in phosphate buffered saline (PBS) to mimic physiological conditions (Fig. 3). Reverse-phase HPLC (RP-HPLC) was used to separate the released lomerizine, which was monitored by UV at 210 nm.[43] The drug loading was also measured by RP-HPLC and was found to be 41 ± 1% w/w. It has been reported that polymeric drug delivery systems often release drug in an initial burst, followed by extended period of slower release, perhaps due to the drug being adsorbed on the particle surface or because of pores and cracks in the polymer matrix.[44] In this case, it would appear that the low solubility of lomerizine results in the saturation of the sink within a few hours. Thus, the release rate fell considerably from this point onwards, but it is also likely that a burst pattern was observed. The dependence of the release rate on pH is likely due to the pH-dependent solubility of lomerizine itself as PMMA is not a pH-responsive polymer, and therefore drug release probably occurs simply by diffusion. Extrapolating from the initial slope gives an indication that the total loaded dose of lomerizine would be released after approximately 5 h, 21 h, and 90 days for pH 5, 6, and 7.4 respectively under ideal sink conditions.

To ensure that the drug carrier was not innately toxic, nanospheres (PMMA and PMMA-*b*-PEG) were incubated with rat pheochromocytoma neural progenitor (PC12) cells and the toxicity of the nanospheres after 24 h determined using a Live/Dead assay (calcein AM and ethidium homodimer-1). No reduction in cell viability ($p > 0.05$) was observed for either type of particle at concentrations up to 500 μg ml^{-1} (Fig. 4a–b). At 1000 μg ml^{-1}, however, PMMA-*b*-PEG particles caused a reduction ($p \leq 0.05$) in cell viability, whereas PMMA particles did not. Therefore, both types of nanospheres were non-toxic at up to 500 μg ml^{-1} as assessed by cell viability relative to control, and differences in measured viabilities are attributed to statistical variation in the samples. Upon incubation for up to 120 h, we did not observe any association with cells for either the PMMA or PMMA-*b*-PEG particles as prepared.

To assess the effectiveness of the stealth surface, nanospheres were combined with branched polyethylenimine (PEI) and incubated with PC12 cells. Polyethylenimine is a synthetic polymer and a common transfection agent;[45–47] the positive charges on PEI assist in association with the plasma

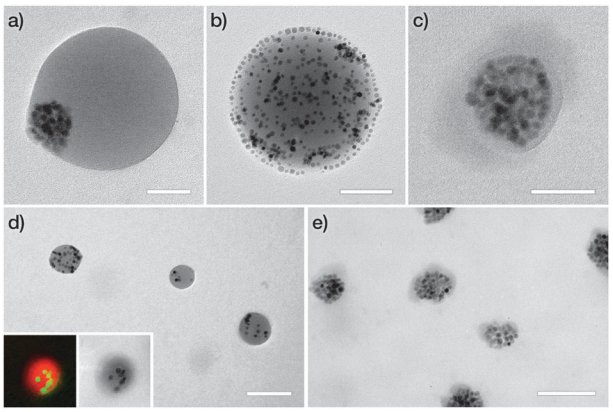

Fig. 2 TEM images of particles prepared from the following hexane/chloroform/acetone solvent systems: (a) PMMA 0 : 1 : 19 (scale bar = 50 nm); (b) PMMA 1 : 2 : 9 (scale bar = 50 nm); (c) PMMA-*b*-PEG 1 : 2 : 9 (scale bar = 50 nm). (d) Corresponding low magnification view of the particles in (b) (scale bar = 100 nm), inset: elemental mapping shows presence of carbon (red) and iron (green). (e) Lower magnification view of particles in (c) (scale bar = 100 nm).

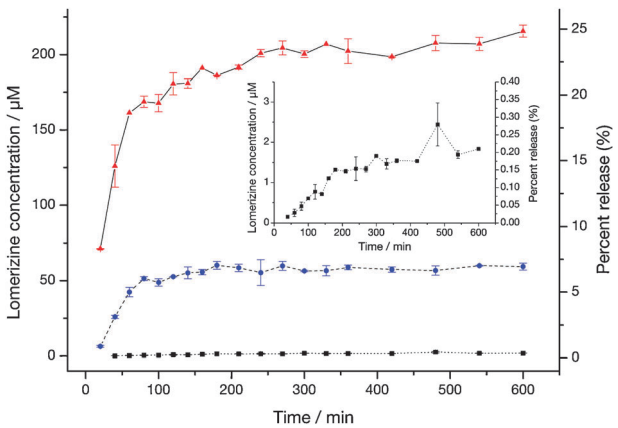

Fig. 3 Release of lomerizine over time at pH 5.0 (red triangles, solid line), pH 6.0 (blue circles, dashed line) and pH 7.4 (black squares, dotted line). All data points are averages of two lomerizine determinations ± SE. The inset shows a magnified scale for release at pH 7.4.

View Article Online

Published on 02 April 2012. Downloaded by Western Kentucky University on 28/10/2014 22:23:45.

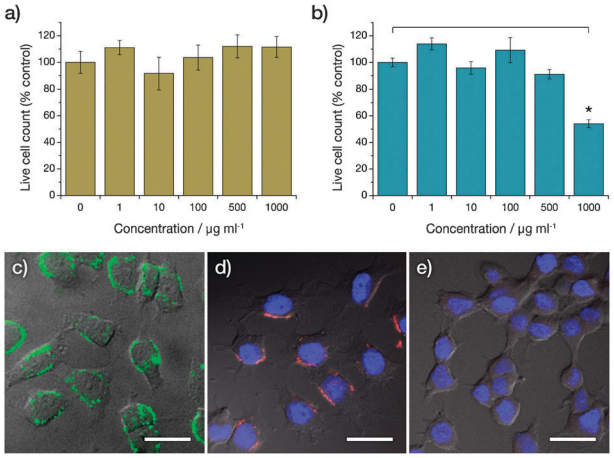

Fig. 4 PC12 cultures incubated with nanospheres. Error bars indicate SE. (a) Viability of PC12 cells incubated for 24 h with PMMA nanospheres (n = 7 per concentration, one-way ANOVA with Bonferroni *post hoc* correction, $p > 0.05$). (b) Viability of PC12 cells incubated for 24 h with PMMA-*b*-PEG nanospheres (n = 7 per concentration, Mann-Whitney U, $p \leq 0.05$ indicated by *). (c) PMMA nanospheres containing pentamethyl BODIPY **3** are associated with cells in the presence of PEI (green = **3**, PMMA nanospheres; DIC overlay, 40 ×/1.25, scale bar = 20 μm). (d) The same is observed for PMMA nanospheres containing BODIPY **4** (red = **4**, PMMA nanospheres, blue = Hoechst, nuclei; DIC overlay, 63 ×/1.40, scale bar = 20 μm). (e) PMMA-*b*-PEG nanoparticles do not associate with cells, even in the presence of PEI (red = **4**, PMMA-*b*-PEG nanospheres, blue = Hoechst, nuclei; DIC overlay, 63 ×/1.40, scale bar = 20 μm).

membrane of cells and may promote endocytosis.[48] When PEI was combined with particles, adhesion of PMMA particles to the cell membrane (Fig. 4c–d) was observed, but particles did not appear to be internalised, probably because PEI was not covalently bound to the nanospheres. On the other hand, stealth PMMA-*b*-PEG nanospheres did not associate with cells, even when PEI was added (Fig. 4e). This suggests that the block copolymer particles sterically hinder the electrostatic attraction of PEI, and that they may be useful as a stealth delivery agent.

Conclusions

We report a method to synthesise nanoparticles containing non-water-soluble dyes and iron oxide nanoparticles that can then be used in aqueous biological experiments. This method is suited to a variety of lipophilic dyes, and we have demonstrated the incorporation of two BODIPYs in the nanospheres without modifying the synthesis procedure. The fluorescent emission of **4** is pH-dependent, with acidification causing a blue-shift in the maximum emission wavelength. The neuroprotective drug lomerizine was also encapsulated in these nanoparticles and exhibited a pH-dependent release profile. The nanoparticles are non-toxic to PC12 cells at concentrations up to 500 μg ml^{-1} and the PEGylated particles did not associate with PC12 cells, even in the presence of the transfection agent PEI. This strategy enables multimodal tracking and delivery of drugs, potentially improving otherwise poor bioavailability of a neuroprotective agent.

Experimental

Materials

Boron trifluoride diethyl etherate, 4-(dimethylamino)benzaldehyde, 2,4-dimethylpyrrole, piperidine, Pluronic F-108, polyethylenimine (M_n 1200, M_w 1300, 50% solution in water), poly(methyl methacrylate) (M_w 120,000 g mol^{-1}), triethylamine, and Tris were obtained from Aldrich, acetyl chloride and triethylamine from Fluka, PMMA-*b*-PEG (M_n 40 000 g mol^{-1} MMA, 11,500 g mol^{-1} PEG, M_w/M_n 1.3) from Polymer Source, Inc., and lomerizine dihydrochloride from LKT Laboratories. Solvents were of analytical grade, except HPLC solvents which were of HPLC grade and filtered (0.2 μm) before use. Hexane was distilled before use, and CH_2Cl_2 was distilled according to standard procedures.[49] Milli-Q water (> 18 MΩ cm) was used in all preparations. Cell culture materials were obtained from Invitrogen unless otherwise stated: RPMI1640, horse serum, fetal bovine serum, penicillin/streptomycin, L-glutamine, non-essential amino acids, sodium pyruvate. Poly(L-lysine) hydrobromide was obtained from Sigma.

BODIPY synthesis

BODIPY **3** was prepared according to literature procedure and characterisation data agrees with that reported for ^{1}H NMR spectrum.[25] The ^{13}C NMR spectrum was not previously reported. ^{13}C NMR (100 MHz, $CDCl_3$, 25 °C): δ = 153.56, 141.41, 140.99, 132.04, 121.20, 17.27, 16.33, 14.39 ppm. The synthesis of dye **4** was adapted from the Knoevenagel method previously reported.[26] BODIPY **3** (127.4 mg, 0.486 mmol) was combined with 4-(dimethylamino)benz aldehyde (81.0 mg, 0.543 mmol) in toluene (10 mL) in the presence of acetic acid (0.4 mL), piperidine (0.38 mL) and molecular sieves. The reaction mixture was heated to reflux for 3 h, purified by column chromatography (silica) eluting with dichloromethane/hexane (7 : 3), affording the desired product BODIPY **4** (33.7 mg, 20% based on recovery of 14 mg of starting BODIPY **3**). ^{1}H NMR (400 MHz, $CDCl_3$, 25 °C): δ = 7.47 (m, 3H), 7.19 (d, J(H,H) = 16 Hz, 1H), 6.68 (m, 3H), 6.04 (s, 1H), 3.01 (s, 6H), 2.60 (s, 3H), 2.55 (s, 3H), 2.46 (s, 3H), 2.42 ppm (s, 3H); ^{13}C NMR (100 MHz, $CDCl_3$, 25 °C): δ = 153.28, 151.47, 150.92, 140.96, 138.87, 138.33, 137.05, 133.55, 131.90, 129.05, 124.78, 120.55, 117.73, 117.75, 114.44, 112.02, 40.24, 29.69, 17.63, 17.20, 16.28, 14.46 ppm; UV/Vis (CH_2Cl_2): $\lambda_{max}(\varepsilon)$ = 591 nm (38300); HR-ESMS calculated for $C_{23}H_{26}BF_2N_3$ 392.2224; found 393.2299 $[M+H]^+$.

Iron oxide nanoparticle synthesis

Magnetite nanoparticles were prepared by decomposition of $Fe(acac)_3$ in benzyl ether, as previously described.[27,28]

Preparation of nanospheres

PMMA (75 mg, M_w 120,000 g mol^{-1}) and iron oxide nanoparticles (5 mg) were dissolved in chloroform and the solvent evaporated *in vacuo* to help solvate the polymer. BODIPY **3** or **4** (5 mg), lomerizine (20 mg) and hexane/chloroform/acetone (6.0 mL, typically 0.5 : 1 : 4.5) were added and all components were dissolved. This mixture was added dropwise with vigorous stirring to an aqueous solution of Pluronic F-108 (1.25 mg mL^{-1}),

 This journal is © The Royal Society of Chemistry and the Centre National de la Recherche Scientifique 2012

View Article Online

Published on 02 April 2012. Downloaded by Western Kentucky University on 28/10/2014 22:23:45.

buffered with 10 mM Tris at pH 9.0. The mixture was then homogenised with a probe-type ultrasonicator for 1 min at low power and stirred overnight under a slow flow of N_2 to evaporate the solvents. The resulting suspension was centrifuged at 3000 *g* for 45 min and the supernatant was passed through a magnetic separation column (Miltenyi Biotec). The collected nanospheres were washed from the column and isolated by centrifugation at 16 000 *g* for 30 min. PEGylated nanospheres were prepared in the same way, using PMMA-*b*-PEG in place of PMMA. Samples were prepared for electron microscopy by air-drying a drop of aqueous dispersed nanospheres on a carbon-coated copper grid; TEM was performed on a JEOL 2100 operated at 120 kV. Magnetometry was performed on a Quantum Design 7 T MPMS instrument, and DLS size and zeta measurements were carried out using a Malvern ZetaSizer Nano.

Relaxometry

Relaxivity data were measured (Bruker minispec mq) at 1.41 T. A Carl-Purcell-Meiboom-Gill (CPMG) spin echo sequence was used to measure T_2. The echo spacing was 1 ms (2000 echoes). An inversion recovery (IR) sequence was used to measure T_1 using 10 inversion times (TI) logarithmically spaced between 10 and 10 000 ms. Nanosphere samples were suspended in water, and data were recorded at 27 °C. The iron content of the samples was determined by ICP-AES after acid digestion.

Determination of lomerizine release

Release experiments were performed in pre-warmed phosphate buffered saline (PBS) at various pH levels (pH 5.0, 6.0 and 7.4). Nanospheres (10 mg) were dispersed in PBS (10 mL) and maintained at 37.0 ± 0.1 °C. The sinks were sampled in duplicate over 10 h; aliquots of 150 μL were transferred to filter tubes (Millipore, Amicon Ultra-0.5, 50 kDa cutoff), centrifuged at 17 000 *g* for 5 min, and analysed by RP-HPLC. No fresh PBS media was introduced into the sinks. Lomerizine concentrations were calculated from a standard curve and were reported as mean values ± SE. The determination of lomerizine by RP-HPLC was adapted from Waki and Ando.[43] The measurements were run on a Waters 2695 separations module coupled with Waters 2489 UV/Vis detector. A C_{18} column (150 × 4.60 mm, 5 μm, 25 ± 5 °C) was used with isocratic elution using a 69 : 31 mixture of acetonitrile and 0.1% w/w potassium phosphate buffer (pH 6) at 10.0 mL min^{-1}, monitoring the eluent at 210 nm. Each sample was run for 13 min and the integrated area of the largest peak between the retention time 9–10 min was used for the calculation of lomerizine concentration. The limit of detection for lomerizine in water at 210 nm was 0.1 mg L^{-1}. The loading of lomerizine in nanospheres (1.69 mg) was determined by adding methanol (1 mL) and sonicating in an ultrasonic cleaning bath (10 min). Samples were left for 1 h, centrifuged to remove nanoparticles (17 000 *g*, 10 min), and analysed by RP-HPLC as above.

Cell culture

Rat phaeochromocytoma (PC12) cells were obtained from the Mississippi Medical Centre (Jackson, MS), and were maintained at 37 °C with 5% CO_2 in RPMI1640 media supplemented with horse serum (10%), fetal bovine serum (5%), penicillin/streptomycin (50 U mL^{-1}, 50 μg mL^{-1}), L-glutamine (2 mM), non-essential amino acids (1%), and sodium pyruvate (1 mM). For confocal microscopy, cells were grown on poly(L-lysine)-coated coverslips, coated by incubation for at least 1 h with poly(L-lysine) hydrobromide (10 μg mL^{-1}). Nanospheres were added at a concentration of 10 μg mL^{-1} and PEI was added at a final dilution of 1 μg mL^{-1} when used. For viability assessments, cells were plated at a density of 2×10^5 mL^{-1} in 96-well plates coated with poly(L-lysine) 24 h prior to experiments. Cells were incubated with nanospheres dispersed in complete media for 24 h, and viability was determined using Live/Dead assay (Invitrogen); briefly, cells were incubated with calcein AM (1 μM) and EthD-1 (2–3 μM) in PBS for 30 min, and then fluorescence was quantified using a spectrophotometer (BMG FluoStar Optima) or cells were counted in four fields of view per well at 20 × magnification (Olympus IX-71) with assessment of approximately 1000 cells per replicate.

We thank Mr B. Padman and the Centre for Microscopy, Characterisation and Analysis at UWA for assistance with electron microscopy, and Dr A. Reeder (UWA) for mass spectrometry analysis. Funding by the Australian Research Council, National Health & Medical Research Council of Australia and the Sir Harry Secombe Trust is graciously acknowledged. MJL appreciates the support of the University of Western Australia (Research Development Award).

Notes and references

1 B. J. Nehilla, P. G. Allen and T. A. Desai, *ACS Nano*, 2008, **2**, 538–544.
2 T. K. Jain, J. Richey, M. Strand, D. L. Leslie-Pelecky, C. A. Flask and V. Labhasetwar, *Biomaterials*, 2008, **29**, 4012–4021.
3 Z. Ali, A. Z. Abbasi, F. Zhang, P. Arosio, A. Lascialfari, M. F. Casula, A. Wenk, W. Kreyling, R. Plapper, M. Seidel, R. Niessner, J. Knoll, A. Seubert and W. J. Parak, *Anal. Chem.*, 2011, **83**, 2877–2882.
4 A. Agrawal, D. H. Min, N. Singh, H. H. Zhu, A. Birjiniuk, G. von Maltzahn, T. J. Harris, D. Y. Xing, S. D. Woolfenden, P. A. Sharp, A. Charest and S. Bhatia, *ACS Nano*, 2009, **3**, 2495–2504.
5 Y. W. Jun, J. H. Lee and J. Cheon, *Angew. Chem., Int. Ed.*, 2008, **47**, 5122–5135.
6 Z. Medarova, W. Pham, C. Farrar, V. Petkova and A. Moore, *Nat. Med.*, 2007, **13**, 372–377.
7 X. X. Meng, J. Q. Wan, M. Jing, S. G. Zhao, W. Cai and E. Z. Liu, *Acta Pharmacol. Sin.*, 2007, **28**, 2019–2026.
8 T. Verrecchia, G. Spenlehauer, D. V. Bazile, A. Murrybrelier, Y. Archimbaud and M. Veillard, *J. Controlled Release*, 1995, **36**, 49–61.
9 Q. Liu, Y. Sun, C. Li, J. Zhou, T. Yang, X. Zhang, T. Yi, D. Wu and F. Li, *ACS Nano*, 2011.
10 M. Huang, W. Wu, J. Qian, D. J. Wan, X. L. Wei and J. H. Zhu, *Acta Pharmacol. Sin.*, 2005, **26**, 1512–1518.
11 M. Socha, P. Bartecki, C. Passirani, A. Sapin, C. Damge, T. Lecompte, J. Barre, F. El Ghazouani and P. Maincent, *J. Drug Targeting*, 2009, **17**, 575–585.
12 S. D. Li and L. Huang, *J. Controlled Release*, 2010, **145**, 178–181.
13 M. F. Zambaux, B. Faivre-Fiorina, F. Bonneau, S. Marchal, J. L. Merlin, E. Dellacherie, P. Labrude and C. Vigneron, *Biomaterials*, 2000, **21**, 975–980.
14 L. L. Ma, P. Jie and S. S. Venkatraman, *Adv. Funct. Mater.*, 2008, **18**, 716–725.
15 Y. F. Tan, P. Chandrasekharan, D. Maity, C. X. Yong, K. H. Chuang, Y. Zhao, S. Wang, J. Ding and S. S. Feng, *Biomaterials*, 2011, **32**, 2969–2978.
16 A. A. Gabizon, *Clin. Cancer Res.*, 2001, **7**, 223–225.

View Article Online

Published on 02 April 2012. Downloaded by Western Kentucky University on 28/10/2014 22:23:45.

17 A. Loudet and K. Burgess, *Chem. Rev.*, 2007, **107**, 4891 and references therein.
18 S. L. Niu, G. Ulrich, R. Ziessel, A. Kiss, P. Y. Renard and A. Romieu, *Org. Lett.*, 2009, **11**, 2049–2052.
19 L. L. Li, J. Y. Han, B. Nguyen and K. Burgess, *J. Org. Chem.*, 2008, **73**, 1963–1970.
20 S. L. Zhu, J. T. Zhang, G. Vegesna, F. T. Luo, S. A. Green and H. Y. Liu, *Org. Lett.*, 2011, **13**, 438–441.
21 M. Brellier, G. Duportail and R. Baati, *Tetrahedron Lett.*, 2010, **51**, 1269–1272.
22 T. Bura, P. Retailleau, G. Ulrich and R. Ziessel, *J. Org. Chem.*, 2011, **76**, 1109–1117.
23 E. Deniz, G. C. Isbasar, O. A. Bozdemir, L. T. Yildirim, A. Siemiarczuk and E. U. Akkaya, *Org. Lett.*, 2008, **10**, 3401–3403.
24 O. Buyukcakir, O. A. Bozdemir, S. Kolemen, S. Erbas and E. U. Akkaya, *Org. Lett.*, 2009, **11**, 4644–4647.
25 B. C. Guo, X. J. Peng, A. J. Cui, Y. K. Wu, M. Z. Tian, L. Z. Zhang, X. Q. Chen and Y. L. Gao, *Dyes Pigm.*, 2007, **73**, 206–210.
26 K. Rurack, M. Kollmannsberger and J. Daub, *Angew. Chem., Int. Ed.*, 2001, **40**, 385–387.
27 S. H. Sun, H. Zeng, D. B. Robinson, S. Raoux, P. M. Rice, S. X. Wang and G. X. Li, *J. Am. Chem. Soc.*, 2004, **126**, 273–279.
28 M. Lattuada and T. A. Hatton, *Langmuir*, 2007, **23**, 2158–2168.
29 F. H. Xu, C. M. Cheng, F. J. Xu, C. F. Zhang, H. Xu, X. Xie, D. Z. Yin and H. C. Gu, *Nanotechnology*, 2009, **20**.
30 V. Di Noto, K. Vezzù, G. A. Giffin, F. Conti and A. Bertucco, *J. Phys. Chem. B*, 2011.
31 N. Lee and T. Hyeon, *Chem. Soc. Rev.*, 2012, **41**, 2575–2589.
32 H. Hara, M. Shimazawa, M. Sasaoka, C. Yamada, Y. Iwakura, T. Sakai, Y. Maeda, T. Yamaguchi, T. Sukamoto and M. Hashimoto, *Clin. Exp. Pharmacol. Physiol.*, 1999, **26**, 870–876.
33 M. Fitzgerald, C. A. Bartlett, L. Evill, J. Rodger, A. R. Harvey and S. A. Dunlop, *Exp. Neurol.*, 2009, **216**, 219–230.
34 M. Fitzgerald, S. C. Payne, C. A. Bartlett, L. Evill, A. R. Harvey and S. A. Dunlop, *Invest. Ophthalmol. Visual Sci.*, 2009, **50**, 5456–5462.
35 M. Selt, C. A. Bartlett, A. R. Harvey, S. A. Dunlop and M. Fitzgerald, *Brain Res. Bull.*, 2010, **81**, 467–471.
36 Z. Karim, A. Sawada, H. Kawakami, T. Yamamoto and T. Taniguchi, *Curr. Eye Res.*, 2006, **31**, 273–283.
37 Y. Ito, S. Nakamura, H. Tanaka, K. Tsuruma, M. Shimazawa, M. Araie and H. Hara, *CNS Neurosci. Ther.*, 2010, **16**, 103–114.
38 N. Toriu, A. Akaike, H. Yasuyoshi, S. Zhang, S. Kashii, Y. Honda, M. Shimazawa and H. Hara, *Exp. Eye Res.*, 2000, **70**, 475–484.
39 H. Yamada, Y. N. Chen, M. Aihara and M. Araie, *Brain Res.*, 2006, **1071**, 75–80.
40 V. Danielisová and M. Chavko, *Exp. Neurol.*, 1998, **149**, 203–208.
41 J. G. Hey, X. P. Chu, J. Seeds, R. P. Simon and Z. G. Xiong, *Stroke*, 2007, **38**, 670–673.
42 E. Sykova, *J. Neural Transm.*, 2004, **112**, 137–147.
43 H. Waki and S. Ando, *J. Chromatogr., Biomed. Appl.*, 1989, **494**, 408–412.
44 X. Huang and C. S. Brazel, *J. Controlled Release*, 2001, **73**, 121–136.
45 O. Boussif, F. Lezoualc'h, M. A. Zanta, M. D. Mergny, D. Scherman, B. Demeneix and J. P. Behr, *Proc. Natl. Acad. Sci. U. S. A.*, 1995, **92**, 7297–7301.
46 S. M. Moghimi, P. Symonds, J. C. Murray, A. C. Hunter, G. Debska and A. Szewczyk, *Mol. Ther.*, 2005, **11**, 990–995.
47 A. Akinc, M. Thomas, A. M. Klibanov and R. Langer, *J. Gene Med.*, 2005, **7**, 657–663.
48 T. Bieber, W. Meissner, S. Kostin, A. Niemann and H. P. Elsasser, *J. Controlled Release*, 2002, **82**, 441–454.
49 W. L. F. Armarego and C. L. L. Chai, *Purification of Laboratory Chemicals*, 5th edn, Elsevier, Burlington, 2003.

 This journal is © The Royal Society of Chemistry and the Centre National de la Recherche Scientifique 2012